Philosophical Magazine A, 2002, Vol. 82, No. 3, 541–551

On the determination of partial dislocation Burgers vectors in fcc lattices and its application to cubic SiC films

U. Kaiser†

Institut fur Festkörperphysik, Friedrich-Schiller-Universitat, Jena D-07743, Max-Wien-Platz 1, Germany

and I. I. Khodos

Institute of Microelectronics Technology and High Purity Materials, Russian Academy of Sciences, Chernogolovka 142432, Russia

[*Received 9 March 2001 and accepted in revised form 18 June 2001*]

Abstract

Cubic SiC layers grown on Si(110) contain a high density of widely spread and intersecting stacking faults. Weak-beam transmission electron microscopy has been used to determine the possible Burgers vectors of both widely spread Shockley partial dislocations and sessile partial dislocations in such films. Partial Shockley dislocations that restrict non-intersecting stacking faults were characterized, and a stacking-fault energy of $0.1\,\mathrm{mJ\,m^{-2}}$ was determined. Edge sessile dislocations with $\frac{1}{6}\langle 110\rangle$ and $\frac{1}{3}\langle 001\rangle$ Burgers vectors were identified at the stacking-fault intersections.

§ 1. Introduction

SiC is a tetrahedrally bonded, classically polytypic IV–IV semiconductor (Baumhauer 1912). More than 200 hexagonal (nH with different periodicities n) and one cubic (3C) SiC polytypes exist. In general, fcc and hcp lattices may be considered as different stacking sequences of close-packed planes that have the same symmetry of atom location. In the fcc lattice all three possible A, B and C positions are occupied. In the hcp lattice the sequence is AB . . . , with the A and B planes shifted relative to one another by $\frac{1}{3}\langle 1\bar{1}00\rangle$. In all other hexagonal polytypes the C position is also occupied and the stacking sequence can be classified according to its hexagonality. In 4H-SiC the stacking sequence is ABCB . . . , corresponding to 75% hexagonality, while in 6H-SiC it is ABCACB . . . , corresponding to 66% hexagonality. The difference between the free energies of the stacking sequences can be small (Limpijumnong and Lamprecht 1998, Fissel 2000), and the stacking sequence can be changed by creating a stacking fault (SF). In fcc crystals, this occurs by the formation of Shockley partial dislocations with Burgers vectors $\mathbf{b}_p$ of the form $\frac{1}{6}\langle 112\rangle$, whereas, in hcp lattices, partial dislocations in the (0001) plane have Burgers vectors of the form $\frac{1}{3}\langle 01\bar{1}0\rangle$.

The equilibrium width of a SF is determined by a balance between the repulsion of two partial dislocations of the same sign and the resulting increase in free energy

† Author for correspondence. Email: kaiser@pinet.uni-jena.de

Philosophical Magazine A ISSN 0141–8610 print/ISSN 1460-6992 online
http://www.tandf.co.uk/journals
DOI: 10.1080/01418610110075500

(Siethoff and Alexander 1964). If the difference between the free energies of polytypes is small, then widely dissociated perfect dislocations and even single partials may be observed, as in ZnS crystals (Zaretskii *et al.* 1983). In SiC, widely dissociated dislocations have been seen in both the cubic phase and the hexagonal phase (Maeda *et al.* 1988, Ning and Pirouz 1996, Hong *et al.* 1999, 2000). The stacking-fault energy (SFE) has been determined for both 4H-SiC (Hong *et al.* 1999) and 6H-SiC (Maeda *et al.* 1988, Hong *et al.* 2000). In 3C-SiC that has been deformed by indentation at a high temperature, widely separated Shockley partial dislocations result from the dissociation of $\frac{1}{2}\langle 110\rangle$-type perfect dislocations in addition to individual Shockley dislocations (Griffiths 1966, Ning and Pirouz 1996). Pirouz *et al.* (1987) studied lattice defects in chemically vapour-deposited 3C-SiC on Si(001).

Although the origin of the electrical activity of dislocations in semiconductors is still not understood (Nakamura 1998), it is known that the electrical states of dislocations in semiconductors depend on their core structure (Ossipyan *et al.* 1986) and influence their optical and electrical properties (Steeds 1989, Schubert *et al.* 1997, Kaiser *et al.* 2000). The present work is devoted to a weak-beam diffraction contrast microscopy study of dislocations in 3C-SiC on Si(110), which has a high density of SFs that form dislocations at their intersections. To enable all possible Burgers vectors to be determined with high accuracy, a particular procedure has been implemented.

§2. Experimental details

Cubic SiC films 1 μm thick were grown epitaxially on to Si(110) by molecular-beam epitaxy (Kaiser *et al.* 1999, Fissel *et al.* 2000). Cross-sectional transmission electron microscopy (TEM) foils with [110] foil normals were prepared using mechanical polishing, dimpling and small-angle Ar-ion milling and examined using a JEM 2000FX transmission electron microscope. Weak-beam TEM images were obtained at several zone axes to determine the Burgers vectors of dislocations. Two $\langle 111\rangle$ zones, four $\langle 112\rangle$ zones and two $\langle 100\rangle$ zones were within the tilt range available (x axis, $\pm 45°$; y axis, $\pm 36°$). The **g** reflections and the zone axes used are summarized in table 1.

Table 1. **g** reflections and zone axes used for the experiments and calculations.

g	Zone axes		
002	110	010	100
200	010		
020	100		
$\bar{1}11$	110	$12\bar{1}$	211
$1\bar{1}1$	110	121	$21\bar{1}$
$2\bar{2}0$	110	111	$11\bar{1}$
$\bar{2}02$	111	121	010
$02\bar{2}$	111	100	211
202	$11\bar{1}$	010	$12\bar{1}$
022	$11\bar{1}$	211	100

§ 3. Burgers vector determination

In order to study dislocations in the cubic 3C-SiC films, we used the well-known $|\mathbf{g}\cdot\mathbf{b}|$ criterion (Hirsch *et al.* 1965). Shockley and sessile partial dislocations were initially distinguished. Individual SFs are bounded by Shockley dislocations, while sessile dislocations are created as a result of the intersection of SFs. For Burgers vector determination, weak-beam contrast was compared with calculated $|\mathbf{g}\cdot\mathbf{b}|$ values, making use of the fact that $|\mathbf{g}\cdot\mathbf{b}|^2$ is proportional to the image intensity (Hirsch *et al.* 1965, Cockayne *et al.* 1969, Cockayne 1972). Calculated $|\mathbf{g}\cdot\mathbf{b}|$ values for Shockley dislocations, which are given in table 2, were used to determine the Burgers vector of each dislocation unambiguously. In practice, some dislocations may exhibit small differences in their $|\mathbf{g}\cdot\mathbf{b}|$ values (e.g. for $|\mathbf{g}\cdot\mathbf{b}| = 0$ and $|\mathbf{g}\cdot\mathbf{b}| = \frac{1}{3}$) and hence small differences in their contrast. Therefore, the procedure was simplified and clarified by first determining the SF plane. The four possible {111} SF planes are defined in table 3, in which $|\mathbf{g}\cdot\mathbf{R}_{SF}|$ values ($\mathbf{R}_{SF}$ is the displacement vector for a SF) are also given. (It should be noted that at [110] the $(1\bar{1}\bar{1})$ and $(\bar{1}11)$ planes can be quickly identified from the selected-area diffraction pattern. The remaining (111) and

Table 2. Calculated $|\mathbf{g}\cdot\mathbf{b}|$ values for Shockley partial dislocations.

SF plane	b	$\mathbf{g}\cdot\mathbf{b}$ for the following g: 002	200	020	$\bar{1}11$	$1\bar{1}1$	$2\bar{2}0$	$\bar{2}02$	$02\bar{2}$	202	022
(111)	$\mathbf{b}_{10} = 1\bar{2}1/6$	$\frac{1}{3}$	$\frac{1}{3}$	$\frac{2}{3}$	$\frac{1}{3}$	$\frac{2}{3}$	1	0	1	$\frac{2}{3}$	$\frac{1}{3}$
	$\mathbf{b}_{11} = 11\bar{2}/6$	$\frac{2}{3}$	$\frac{1}{3}$	$\frac{1}{3}$	$\frac{1}{3}$	$\frac{1}{3}$	0	1	1	$\frac{1}{3}$	$\frac{1}{3}$
	$\mathbf{b}_{12} = \bar{2}11/6$	$\frac{1}{3}$	$\frac{2}{3}$	$\frac{1}{3}$	$\frac{2}{3}$	$\frac{1}{3}$	1	1	0	$\frac{1}{3}$	$\frac{2}{3}$
$(1\bar{1}1)$	$\mathbf{b}_7 = 21\bar{1}/6$	$\frac{1}{3}$	$\frac{2}{3}$	$\frac{1}{3}$	$\frac{1}{3}$	0	$\frac{1}{3}$	1	$\frac{2}{3}$	$\frac{1}{3}$	0
	$\mathbf{b}_1 = 121/6$	$\frac{1}{3}$	$\frac{1}{3}$	$\frac{2}{3}$	$\frac{1}{3}$	0	$\frac{1}{3}$	0	$\frac{1}{3}$	$\frac{2}{3}$	1
	$\mathbf{b}_3 = \bar{1}12/6$	$\frac{2}{3}$	$\frac{1}{3}$	$\frac{1}{3}$	$\frac{2}{3}$	0	$\frac{2}{3}$	1	$\frac{1}{3}$	$\frac{1}{3}$	1
$(11\bar{1})$	$\mathbf{b}_4 = \bar{1}21/6$	$\frac{1}{3}$	$\frac{1}{3}$	$\frac{2}{3}$	$\frac{2}{3}$	$\frac{1}{3}$	1	$\frac{2}{3}$	$\frac{1}{3}$	0	1
	$\mathbf{b}_8 = 2\bar{1}1/6$	$\frac{1}{3}$	$\frac{2}{3}$	$\frac{1}{3}$	$\frac{1}{3}$	$\frac{2}{3}$	1	$\frac{1}{3}$	$\frac{2}{3}$	1	0
	$\mathbf{b}_2 = 112/6$	$\frac{2}{3}$	$\frac{1}{3}$	$\frac{1}{3}$	$\frac{1}{3}$	$\frac{1}{3}$	0	$\frac{1}{3}$	$\frac{1}{3}$	1	1
$(\bar{1}11)$	$\mathbf{b}_5 = 211/6$	$\frac{1}{3}$	$\frac{2}{3}$	$\frac{1}{3}$	0	$\frac{1}{3}$	$\frac{1}{3}$	$\frac{1}{3}$	0	1	$\frac{2}{3}$
	$\mathbf{b}_9 = 1\bar{1}2/6$	$\frac{2}{3}$	$\frac{1}{3}$	$\frac{1}{3}$	0	$\frac{2}{3}$	$\frac{2}{3}$	$\frac{1}{3}$	1	1	$\frac{1}{3}$
	$\mathbf{b}_6 = 12\bar{1}/6$	$\frac{1}{3}$	$\frac{1}{3}$	$\frac{2}{3}$	0	$\frac{1}{3}$	$\frac{1}{3}$	$\frac{2}{3}$	1	0	$\frac{1}{3}$

Table 3. Calculated $|\mathbf{g}\cdot\mathbf{R}_{SF}|$values for SFs ($\mathbf{R}_{SF}$ is the displacement vector).

SF plane number	SF planes	$\mathbf{R}_{SF}$	$\mathbf{g}\cdot\mathbf{R}_{SF}$ for the following g: $2\bar{2}0$	$\bar{2}02$	$02\bar{2}$	202	022
1	$(1\bar{1}1)$	$\frac{1}{3}[1\bar{1}1]$	$\frac{4}{3}$	0	$\frac{4}{3}$	$\frac{4}{3}$	0
2	$(11\bar{1})$	$\frac{1}{3}[11\bar{1}]$	0	$\frac{4}{3}$	$\frac{4}{3}$	0	0
3	$(\bar{1}11)$	$\frac{1}{3}[\bar{1}11]$	$\frac{4}{3}$	$\frac{4}{3}$	0	0	$\frac{4}{3}$
4	(111)	$\frac{1}{3}[111]$	0	0	0	$\frac{4}{3}$	$\frac{4}{3}$

$(11\bar{1})$ planes must be selected by observing changes in SF projection width while tilting to [111] or $[11\bar{1}]$ poles.) For a particular Shockley dislocation, knowledge of the SF plane reduces the number of possible Burgers vectors from 12 to three, from which the correct Burgers vector can be identified using the reflections given in table 2.

For sessile partial dislocations, nine stable dislocations can result from the reaction between Shockley partials: six with $\frac{1}{6}\langle 110\rangle$ and three with $\frac{1}{3}\langle 001\rangle$ Burgers vectors. Table 4 shows the reactions that lead to their creation. For each pair of intersecting $\{111\}$ planes, two reactions between Shockley partials lying in these

Table 4. Formation of partial sessile dislocations from partial Shockley dislocations at the intersection of SFs lying in planes 1–4 (see table 3) in the fcc lattice.

Plane of intersecting SFs	Reactions of Shockley dislocations	Burgers vector of resulting sessile partial dislocation
1×2	$\mathbf{b}_1-\mathbf{b}_2$ or $-\mathbf{b}_3+\mathbf{b}_4$	$\frac{1}{6}[01\bar{1}]$
3×1	$\mathbf{b}_5-\mathbf{b}_1$ or $-\mathbf{b}_6+\mathbf{b}_7$	$\frac{1}{6}[1\bar{1}0]$
2×3	$\mathbf{b}_2-\mathbf{b}_5$ or $-\mathbf{b}_8+\mathbf{b}_9$	$\frac{1}{6}[\bar{1}01]$
3×4	$\mathbf{b}_9-\mathbf{b}_{10}$ or $\mathbf{b}_6-\mathbf{b}_{11}$	$\frac{1}{6}[011]$
2×4	$\mathbf{b}_4-\mathbf{b}_{12}$ or $\mathbf{b}_8-\mathbf{b}_{10}$	$\frac{1}{6}[110]$
1×4	$\mathbf{b}_3-\mathbf{b}_{12}$ or $\mathbf{b}_7-\mathbf{b}_{11}$	$\frac{1}{6}[101]$
1×3	$\mathbf{b}_1-\mathbf{b}_6$ or $\mathbf{b}_5-\mathbf{b}_7$	$\frac{1}{3}[001]$
2×4	$\mathbf{b}_4+\mathbf{b}_{10}$ or $\mathbf{b}_8+\mathbf{b}_{12}$	
2×1	$\mathbf{b}_2-\mathbf{b}_3$ or $\mathbf{b}_1-\mathbf{b}_4$	$\frac{1}{3}[100]$
3×4	$\mathbf{b}_6+\mathbf{b}_{10}$ or $\mathbf{b}_9+\mathbf{b}_{11}$	
2×3	$\mathbf{b}_2-\mathbf{b}_9$ or $\mathbf{b}_5-\mathbf{b}_8$	$\frac{1}{3}[010]$
1×4	$\mathbf{b}_3+\mathbf{b}_{11}$ or $\mathbf{b}_7+\mathbf{b}_{12}$	

Table 5. Calculated $|\mathbf{g}\cdot\mathbf{b}|$ values for sessile partial dislocations.

b vector		$\lvert\mathbf{g}\cdot\mathbf{b}\rvert$ for the following									
Type	Direction	002	200	020	$\bar{1}11$	$1\bar{1}1$	$\bar{2}20$	$\bar{2}02$	$02\bar{2}$	202	022
$\frac{1}{6}\langle 011\rangle$	$01\bar{1}/6$	$\frac{1}{3}$	0	$\frac{1}{3}$	0	$\frac{1}{3}$	$\frac{1}{3}$	$\frac{1}{3}$	$\frac{2}{3}$	$\frac{1}{3}$	0
	$1\bar{1}0/6$	0	$\frac{1}{3}$	$\frac{1}{3}$	$\frac{1}{3}$	$\frac{1}{3}$	$\frac{2}{3}$	$\frac{1}{3}$	$\frac{1}{3}$	$\frac{1}{3}$	$\frac{1}{3}$
	$\bar{1}01/6$	$\frac{1}{3}$	$\frac{1}{3}$	0	$\frac{1}{3}$	0	$\frac{1}{3}$	$\frac{2}{3}$	$\frac{1}{3}$	0	$\frac{1}{3}$
	$011/6$	$\frac{1}{3}$	0	$\frac{1}{3}$	$\frac{1}{3}$	0	$\frac{1}{3}$	$\frac{1}{3}$	0	$\frac{1}{3}$	$\frac{2}{3}$
	$110/6$	0	$\frac{1}{3}$	$\frac{1}{3}$	0	0	0	$\frac{1}{3}$	$\frac{1}{3}$	$\frac{1}{3}$	$\frac{1}{3}$
	$101/6$	$\frac{1}{3}$	$\frac{1}{3}$	0	0	$\frac{1}{3}$	$\frac{1}{3}$	0	$\frac{1}{3}$	$\frac{2}{3}$	$\frac{1}{3}$
$\frac{1}{3}\langle 001\rangle$	$001/3$	$\frac{2}{3}$	0	0	$\frac{1}{3}$	$\frac{1}{3}$	0	$\frac{2}{3}$	$\frac{2}{3}$	0	$\frac{2}{3}$
	$010/3$	0	0	$\frac{2}{3}$	$\frac{1}{3}$	$\frac{1}{3}$	$\frac{2}{3}$	0	$\frac{2}{3}$	$\frac{2}{3}$	$\frac{2}{3}$
	$100/3$	0	$\frac{2}{3}$	0	$\frac{1}{3}$	$\frac{1}{3}$	$\frac{2}{3}$	$\frac{2}{3}$	0	$\frac{2}{3}$	0

planes can lead to the creation of the same dislocation with a Burgers vector of the form $\frac{1}{6}\langle 110\rangle$. Two other reactions lead to the formation of a $\frac{1}{3}\langle 001\rangle$ dislocation. The two types of Burgers vector can be distinguished by comparing experimental contrast with the $|\mathbf{g}\cdot\mathbf{b}|$ values given in table 5.

§ 4. Results and discussion

The 3C-SiC samples studied contain a high density of SFs (of the order of 10^8–$10^9\,\mathrm{cm}^{-2}$), numerous partial glide dislocations that restrict 'non-intersecting' SFs (Shockley dislocations), and sessile dislocations at SF intersections.

4.1. *Shockley dislocations*

Figures 1 (*a*) and (*b*) show individual SFs that are bounded by Shockley partial dislocations and denoted 1, 2 and 3. The SFs labelled 1 and 2, which show remarkably non-uniform width, are visible using $\bar{1}11$, $1\bar{1}1$ and 022 reflections (figures 1 (*a*)–(*c*)) but invisible using $2\bar{2}0$ and $\bar{2}02$ reflections (figures 1 (*d*) and (*e*)). With reference to table 3, their displacement vector $\mathbf{R}_{\mathrm{SF}}$ is $\frac{1}{3}[111]$ (the plane of the SF is therefore the (111) plane). The three $\frac{1}{6}\langle 112\rangle$ Burgers vectors of the Shockley dislocations bounding the SFs in the (111) plane are listed in table 2. In figure 1 the partials bounding the SFs 1 and 2 are labelled a–d. Comparing their visibility using all five reflections, it is clear that partials a and c have strong contrast only in figures 1 (*d*) and (*e*). In addition, the SF disappears in figures 2 (*d*) and (*e*), meaning that $|\mathbf{g}\cdot\mathbf{b}|$ is an integer. By comparison with table 2, the vector $\frac{1}{6}[\bar{2}11]$ can be selected for partials a and c because of their strong contrast ($|\mathbf{g}\cdot\mathbf{b}| = 1$) when using $2\bar{2}0$ and $\bar{2}02$ reflections. This result agrees with the strong contrast of dislocations a and c in figures 1 (*a*)–(*c*) for reflections $\bar{1}11$ and 022, for which $|\mathbf{g}\cdot\mathbf{b}|$ is equal to $\frac{2}{3}$ (see table 2). For the two other possible Burgers vectors, $|\mathbf{g}\cdot\mathbf{b}|$ is $\frac{1}{3}$, corresponding to weak contrast.

An analogous approach for dislocations b and d shows that their Burgers vector is $\frac{1}{6}[1\bar{2}1]$, for which the dislocations are invisible using the $\bar{2}02$ reflection (figure 1 (*e*)). Both dislocations exhibit strong contrast using the $1\bar{1}1$ reflection (table 2), which corresponds to a calculated $|\mathbf{g}\cdot\mathbf{b}|$ value of $\frac{2}{3}$.

The SF labelled 3 (upper left corner of figure 1), which is bounded by Shockley dislocations e and f, shows a more uniform splitting width. The projection width suggests that the SF lies in a different plane from the SFs 1 and 2. This must be the $(11\bar{1})$ plane because the SF is invisible using 022 and $2\bar{2}0$ reflections (table 3). Further evidence is provided by the change in SF projection width observed on tilting the sample (see § 3). The same Burgers vector determination procedure shows that, for the SF labelled 3, $\mathbf{b} = \frac{1}{6}[112]$ for Shockley dislocation e and $\frac{1}{6}[\bar{1}21]$ for f.

Shockley partials either can be created through the dissociation of a perfect dislocation as in $\frac{1}{2}[011] \rightarrow \frac{1}{6}[112] + \frac{1}{6}[\bar{1}21]$ or can originate as a result of a change in $\{111\}$ stacking sequence. The wide range of SF widths results from internal stresses during film growth. The interaction between partial dislocations can be comparable with their interaction with such stresses, as for the case of widely spread SFs. Applying the formula usually used for dissociated dislocations under equilibrium conditions (Hirth and Lothe 1968) to the most wide SFs observed in the samples shows that the SFE is as low as $0.1\,\mathrm{mJ\,m^{-2}}$. The SFE determined in this work does not necessarily contradict the value of approximately $0.2\,\mathrm{mJ\,m^{-2}}$ estimated from images of dissociated dislocations in deformed 3C-SiC (Ning and Pirouz 1996). The SFE for cubic SiC is lower than that determined for 6H-SiC ($2.5\,\mathrm{mJ\,m^{-2}}$ (Maeda *et al.* 1988) and $2.9 \pm 0.5\,\mathrm{mJ\,m^{-2}}$ (Hong *et al.* 2000)) and 4H-

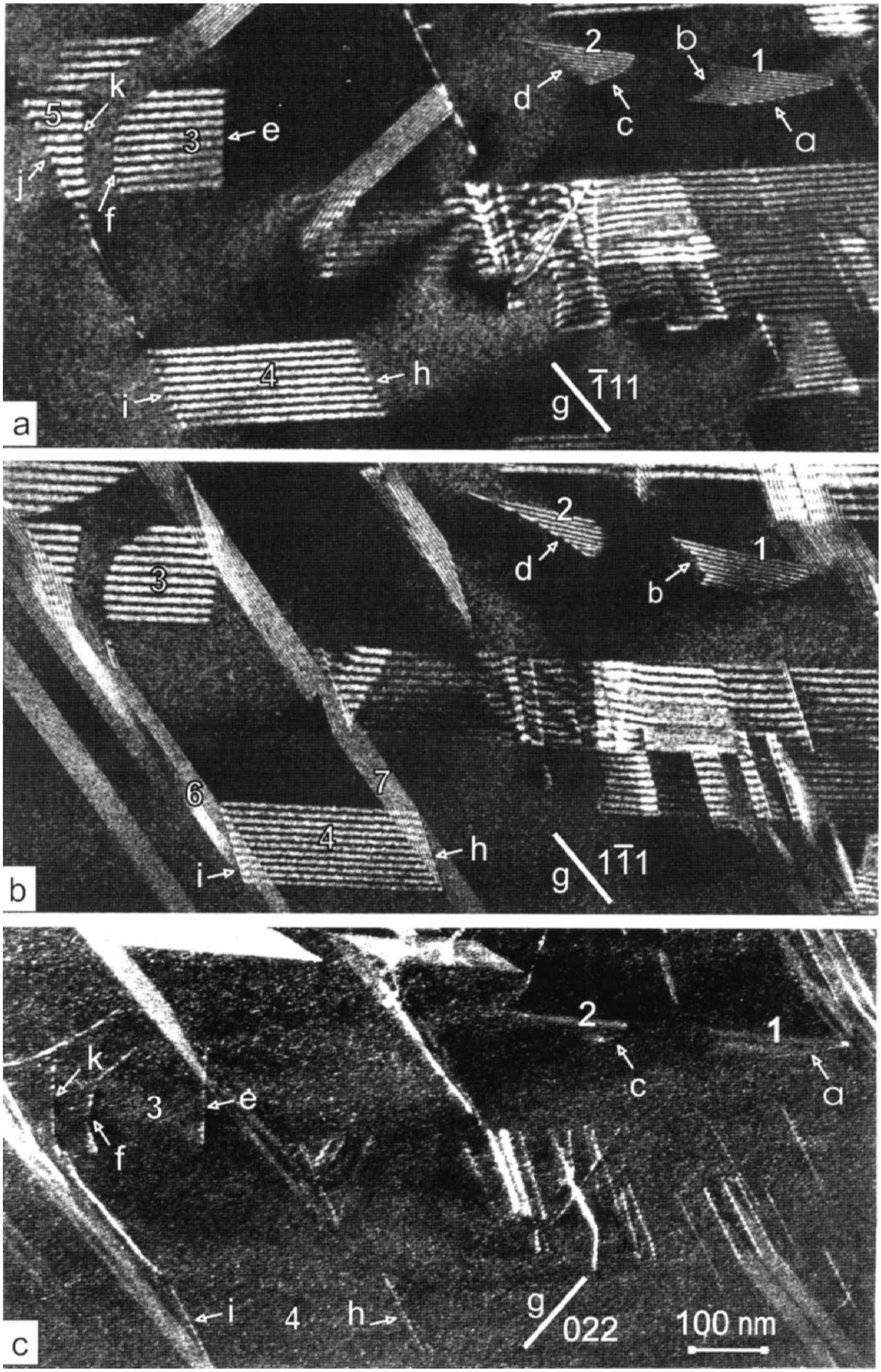

Figure 1. Weak-beam images recorded near the (*a*) $[12\bar{1}]$, (*b*) $[21\bar{1}]$, (*c*) $[11\bar{1}]$, and (*d*), (*e*) [111] zone axes with reflections as denoted, showing Shockley partial dislocations a, b (SF labelled 1), c, d (SF labelled 2), e, f (SF labelled 3), k (SF labelled 5) and sessile partial dislocations h, i (SF labelled 4) and j (SF labelled 5) at the intersections of SFs 4 and 5 with SFs 6 and 7.

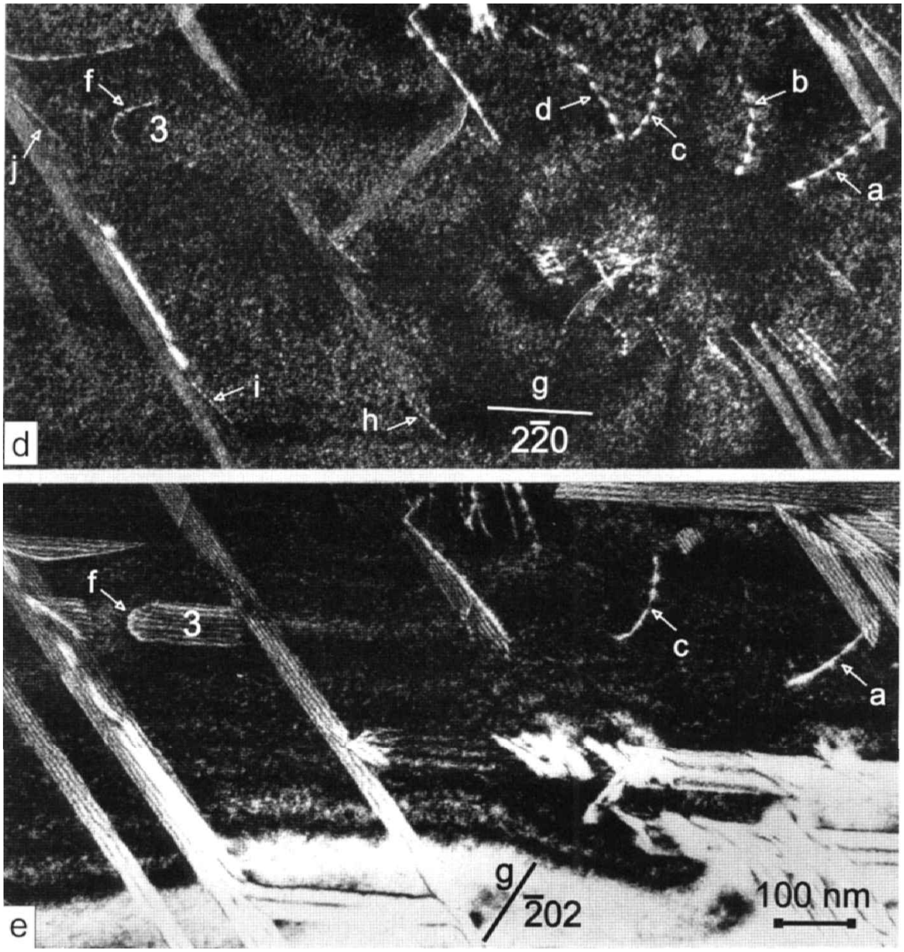

Figure 1. (*Continued*)

SiC ($14.7 \pm 2.5\,\mathrm{mJ\,m^{-2}}$ (Hong *et al.* 1999)), in accordance with the lower stability of the cubic phase compared with the hexagonal polytypes, as calculated by Limpijumnong and Lamprecht (1998), Käckell *et al.* (1999) and Fissel (2000).

4.2. *Sessile partial dislocations*

SFs are often very wide and intersect with SFs in other $\{111\}$ planes (see the SF labelled 4 in figure 1 and the SFs in figure 2), producing sessile partial dislocations at their intersections. There are two types of stable Burgers vector for sessile dislocations in a fcc lattice, both of which are present in the 3C-SiC films studied.

In figure 2, intersecting SFs that create sessile partial dislocations are shown for different reflections. We now describe the determination of the Burgers vectors of the sessile dislocations labelled m and n. In figure 3 (*a*), the SFs that create dislocations m and n (denoted as SF1 to SF4) are shown schematically (SF1 and SF2 lie in $(11\bar{1})$, while SF3 and SF4 lie in $(1\bar{1}1)$; these planes are denoted 2 and 1 respectively in table 3). As seen in table 4, four reactions are possible between four Shockley partials,

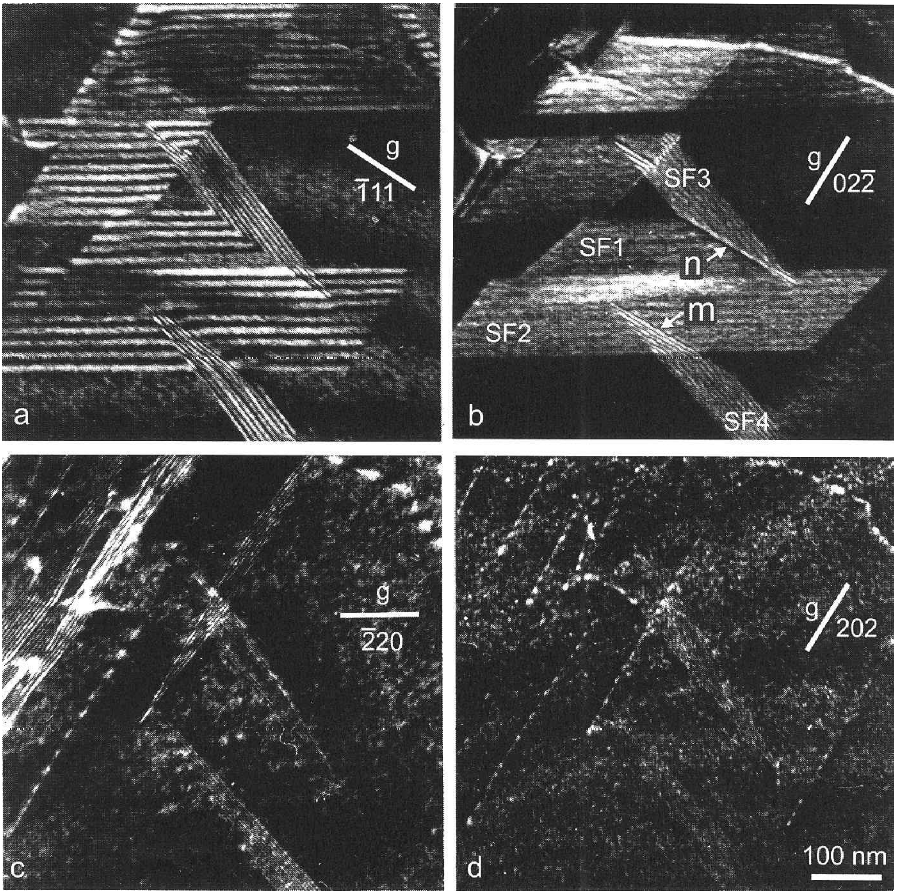

Figure 2. Weak-beam images showing intersecting SFs (labelled SF1 to SF4) creating $\frac{1}{6}\langle 110\rangle$ sessile partial dislocations (labelled m and n) taken using (*a*) $\bar{1}11$, (*b*) $02\bar{2}$, (*c*) $2\bar{2}0$ and (*d*) 202 reflections.

leading to sessile dislocation formation with $\frac{1}{6}\langle 011\rangle$ and $\frac{1}{3}\langle 001\rangle$ Burgers vectors, that is

$$\mathbf{b}_1 - \mathbf{b}_2 = \mathbf{b}_4 + \mathbf{b}_3 = \tfrac{1}{6}[01\bar{1}],$$

$$\mathbf{b}_2 - \mathbf{b}_3 = \mathbf{b}_1 - \mathbf{b}_4 = \tfrac{1}{3}[100].$$

These reactions are shown schematically in figure 3 (*b*) (the tetrahedron is the well-known Thompson tetrahedron), in which the directions of the sessile Burgers vectors are shown using bold dotted lines. Both dislocations are clearly visible using the $02\bar{2}$ reflection (figure 2 (*b*)), and hence (see table 5) their Burgers vector is $\mathbf{b} = \frac{1}{6}[01\bar{1}]$ ($|\mathbf{g}\cdot\mathbf{b}| = \frac{2}{3}$) and not $\mathbf{b} = \frac{1}{3}[100]$ ($|\mathbf{g}\cdot\mathbf{b}| = 0$). This conclusion is consistent with the invisibility of the dislocations using reflections $2\bar{2}0$ and 202 (figures 2 (*c*) and (*d*)), in accordance with the calculation of a low $|\mathbf{g}\cdot\mathbf{b}|$ value of $\frac{1}{3}$ (table 5). (For $\mathbf{b} = \frac{1}{3}[100]$, this value is larger ($\mathbf{g}\cdot\mathbf{b}| = \frac{2}{3}$)).

We now determine the Burgers vector of dislocations i and h in figure 1, which are created at the intersections of SF4 with the parallel SF6 and SF7 (figure 4). SF4

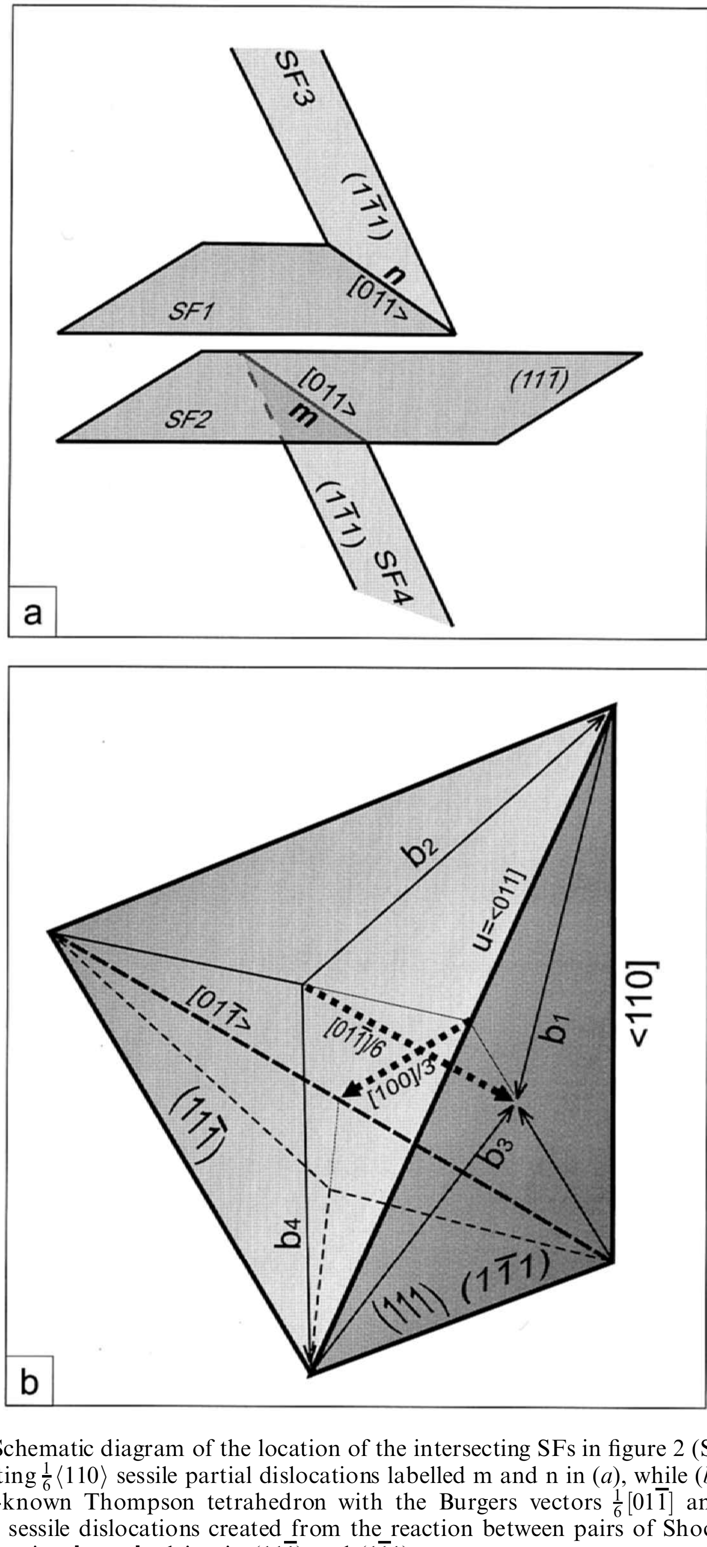

Figure 3. Schematic diagram of the location of the intersecting SFs in figure 2 (SF1 to SF4), creating $\frac{1}{6}\langle 110\rangle$ sessile partial dislocations labelled m and n in (*a*), while (*b*) shows the well-known Thompson tetrahedron with the Burgers vectors $\frac{1}{6}[01\bar{1}]$ and $\frac{1}{3}[100]$ of edge sessile dislocations created from the reaction between pairs of Shockley partial dislocation $\mathbf{b}_1$ to $\mathbf{b}_4$ lying in $(11\bar{1})$ and $(1\bar{1}1)$.

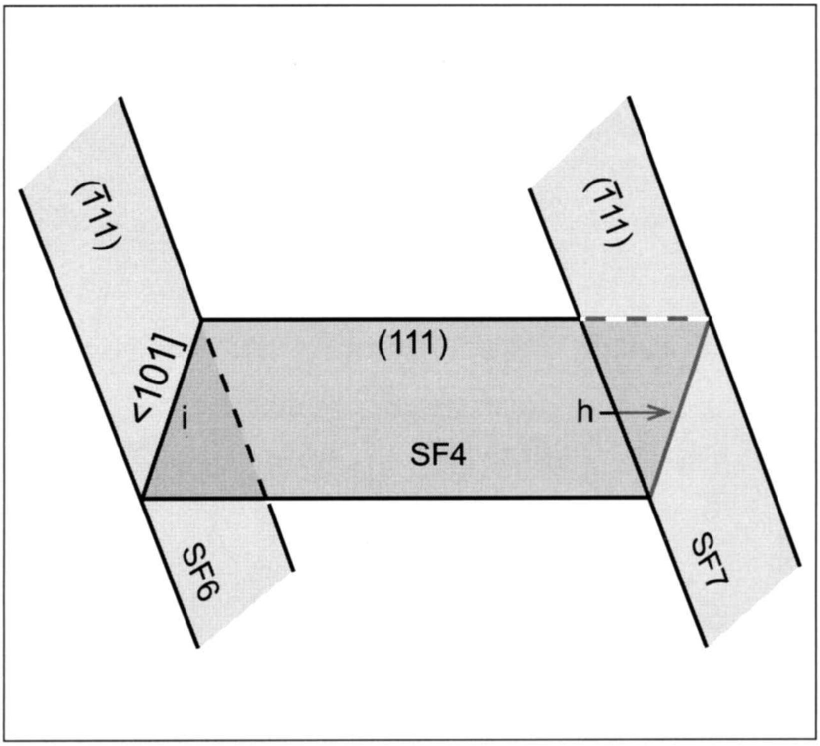

Figure 4. Schematic diagram of the location of the intersection of SF4 with SF6 and SF7 (see figure 2), creating $\frac{1}{3}\langle 100\rangle$ sessile partial dislocations labelled i and h.

lies in the $(\bar{1}\bar{1}1)$ plane, while the two parallel SFs are in the $(1\bar{1}\bar{1})$ plane. In accordance with table 4, the following reactions between dislocations with Burgers vectors $\mathbf{b}_2$, $\mathbf{b}_4$ and $\mathbf{b}_8$ (in $(11\bar{1})$, denoted 2 in table 3) and $\mathbf{b}_5$, $\mathbf{b}_6$ and $\mathbf{b}_9$ (in $(1\bar{1}\bar{1})$, denoted 3 in table 3) need to be considered:

$$\mathbf{b}_2 - \mathbf{b}_5 = \mathbf{b}_9 - \mathbf{b}_8 = \tfrac{1}{6}[\bar{1}01],$$

$$\mathbf{b}_2 - \mathbf{b}_9 = \mathbf{b}_5 - \mathbf{b}_8 = \tfrac{1}{3}[010].$$

As i and h are both invisible using the $\bar{2}02$ reflection (figure 1 (*e*)), $\mathbf{b} = \frac{1}{3}[010]$ ($|\mathbf{g}\cdot\mathbf{b}| = 0$). This conclusion is consistent with the contrast observed using the 022 and $2\bar{2}0$ reflections (figures 1 (*c*) and (*d*)) in which $|\mathbf{g}\cdot\mathbf{b}| = \frac{2}{3}$ for $\mathbf{b} = \frac{1}{3}[010]$ whereas for $\mathbf{b} = [\bar{1}01]$, $|\mathbf{g}\cdot\mathbf{b}| = \frac{1}{3}$.

In the upper left corner of figures 1 (*a*)–(*e*), the SF labelled 5 is bounded by one sessile partial dislocation j with $\mathbf{b} = \frac{1}{3}[010]$ and one Shockley partial k with $\mathbf{b} = \frac{1}{6}[112]$.

It should be noted that sessile dislocations with $\frac{1}{6}\langle 110\rangle$ or $\frac{1}{3}\langle 100\rangle$ Burgers vectors are of edge character. As the dislocation core structure and its energy level in the bandgap are in general defined by the orientation of the dislocation relative to its Burgers vector, sessile dislocations may be expected to show more distinct peaks in optical spectra than glide dislocations as the latter have a wider range of orientations relative to their Burgers vectors. The electrical and optical activities of Shockley and sessile partial dislocations have not yet been discussed in the literature for SiC.

§ 5. Conclusions

The defect structure of 3C-SiC films consists of a high density of SFs, with numerous partial glide dislocations that restrict non-intersecting SFs, and sessile dislocations that form at SF intersections. SFs that are bounded by Shockley partial dislocations have widths of up to 2 μm, corresponding to SFEs down to $0.1\,\mathrm{mJ\,m^{-2}}$. Sessile partial dislocations are created at the intersection of SFs on different $\{111\}$ planes and have $\frac{1}{3}\langle 100\rangle$ and $\frac{1}{6}\langle 110\rangle$ Burgers vectors that lie perpendicular to the corresponding $\langle 110\rangle$ dislocation line direction.

A similar analysis will be especially useful for the study of undeformed thin films, in which all possible Burgers vectors are expected.

Acknowledgements

The authors acknowledge financial support from the Sonderforschungsbereich 196 and the Transform project 01BM804/5. We would also like to express our thanks to M. N. Kovalchuk for her help with contrast interpretation and Dr A. Fissel for providing the SiC/Si specimen. The authors are grateful to Dr P. D. Brown and Dr R. Dunin-Borkowski for careful reading of the manuscript.

References

Baumhauer, H., 1912, *Z. Kristallogr.*, **50**, 33.
Cockayne, D. J. H., 1972, *Z. Naturf.* (a), **27**, 452.
Cockayne, D. J. H., Ray, I. L. F., and Whelan, M. J., 1969, *Phil. Mag.* A, **20**, 1265.
Fissel, A., 2000, *J. Cryst. Growth*, **212**, 438.
Fissel, A., Schroter, B., Kaiser, U., and Richter, W., 2000, *Appl. Phys. Lett.*, **73**, 2418.
Griffiths, L. B., 1966, *J. Phys. Chem. Solids*, **27**, 257.
Hirsch, P. B., Howie, A., Nicholson, R., Pashley, D. W., and Whelan, M. J., 1965, *Electron Microscopy of Thin Crystals* (London: Butterworths).
Hirth, J. P., and Lothe, J., 1968, *Theory of Dislocations* (New York: McGraw-Hill).
Hong, M. H., Samant, A. V., Orlov, V., Farber, B., Kisielowski, C., and Pirouz, P., 1999, *Mater. Res. Soc. Symp. Proc.*, **572**, 498.
Hong, M. H., Samant A. V., and Pirouz P., 2000, *Phil. Mag.* A, **80**, 919.
Käckell, P., Furthmüller, J., and Bechstedt, F., 1999, *Phys. Rev.* B, **58**, 1326.
Kaiser, U., Gruzintsev, A. N., Khodos, I. I., Richter, W., 2000, *Inorg. Mater.*, **36**, 720.
Kaiser, U., Khodos, I. I., Brown, P. D., Chuvilin, A., Albrecht, M., Humphreys, C. J., Fissel, A., and Richter W., 1999 *J. Mater. Res.*, **14**, 3226.
Limpijumnong, S., and Lamprecht, W. R. L., 1998, *Phys. Rev.*, **57**, 12 017.
Maeda, K., Suzuki, K., Fujita, S., Ichihara, M., and Hyodo, S., 1988, *Phil. Mag.* A, **57**, 573.
Nakamura, S., 1998, *Group III Nitride Semiconductor Compounds*, edited by B. Gil, (Oxford University Press), p. 391.
Ning, X. J., and Pirouz, P., 1996, *J. Mater. Res.*, **11**, 884.
Pirouz, P., Chorey, C. M., Cheng, T. T., and Powell, J. A., 1987, *Inst. Phys. Conf. Ser.*, **87**, 175.
Ossipyan, Yu. A., Petrenko, V. T., Zaretskii, A. V., and Witworth, R., 1986, *Adv. Phys.*, **35**, 115.
Schubert, E. F., Goepfert, L. D., and Redwing, J. M., 1997, *Appl. Phys. Lett.*, **71**, 3224.
Siethoff, H., and Alexander, H., 1964, *Phys. Stat. sol.*, **6**, K165.
Steeds, J. W., 1989, *Inst. Phys. Conf. Ser.,* No 104, p. 199.
Zaretskii, A. V., Ossipyan, Yu. A., Petrenko, V. F., Strukova, G. K., and Khodos, I. I., 1983, *Phil. Mag.* A, **48**, 279.